Table VII. Apparent Dissociation Constants for $MgHCO_3^+$ and $MgCO_3^0$

| $\mu$ | $pK_1$ | $p(1/K_2)$ | $pK_3$ |
|---|---|---|---|
| 0.00[a] | 1.23 | 8.08 | 3.24 |
| 0.0398 | 1.17 | 8.21 | 3.29 |
| 0.0665 | 1.08 | 8.08 | 3.32 |
| 0.0852 | 1.00 | 7.91 | 3.42 |
| 0.102 | 0.968 | 7.86 | 3.43 |
| 0.116 | 1.04 | 8.10 | 3.27 |

[a] Extrapolated by linear regression statistics.

Table VIII. Apparent $pK_1'$ Values Obtained from the $MgCl_2$–$CO_2$ System

| $MgCl_2$, $M$ | pH | $\mu$ | $pK_1'$ |
|---|---|---|---|
| 0.006 | 3.907 | 0.018 | 1.29 |
| 0.0075 | 3.903 | 0.022 | 1.27 |
| 0.010 | 3.899 | 0.030 | 1.26 |
| 0.0233 | 3.877 | 0.070 | 1.23 |
| 0.035 | 3.860 | 0.115 | 1.25 |
| 0.050 | 3.845 | 0.150 | 1.22 |
| 0.060 | 3.834 | 0.180 | 1.23 |
| 0.070 | 3.824 | 0.210 | 1.25 |

and correcting for the vapor pressure of water and the effect of salt on Henry's law constant, Hostetler's $pK_1 = 0.95$ becomes $pK_1 = 1.21$ at $\mu = 0.07$ and more comparable to the data presented in Table VII. Näsänen's data (*11*), on the other hand, are not reliable. He worked at pH's of about 11, and did not take into account the presence of $MgOH^+$ and $MgCO_3^0$ species. This work (Tables II to VI) and Greenwald's (*3*) show that the $MgCO_3^0$ can become a significant portion of the total Mg as the pH is increased.

The $p(1/K_2)$ at $\mu = 0$ is 8.08 and 8.05 at $\mu = 0.15$ vs. Greenwald's 7.77 at 0.15; at $\mu = 0.07$, $p(1/K_2) = 8.06$ vs. Hostetler's 7.86. In Greenwald's method, he had to assume a value for $1/K_2$ to get his $K_1$'s to compare with each other in the electrotitrimetric method. Hostetler (*8*) used different dissociation constants. His $pK_3$ of 3.40 was obtained from Garrels et al. (*2*). A $pK_3$ of 3.24 was derived in this study at $\mu = 0$. By use of extrapolation in Table VII $pK_3 = 3.38$ at $\mu = 0.15$, which is the ionic strength above Garrels et al. (*2*), obtained consistent values for $pK_3$.

Raaflaub's (*12*) value for $pK_3 = 2.97$ was determined by estimating $Mg^{2+}$ indirectly by measurements of the Mg-eriochrome Black-T complex in solution within a narrow pH range 9.4 to 9.7. At present, a combination of the electrometric determination of $(H^+)$ and $(Mg^{2+})$ activities and the theoretical approach presented in this paper appears to be the most direct method for estimating the different magnesium carbonate complexes. The $K$ values compare favorably with other independent methods, and in addition, apparent dissociation constants can be obtained at a specified ionic strength.

## ACKNOWLEDGMENT

The author thanks Barbara A. Rasnick for the chemical analyses.

## LITERATURE CITED

(1) Garrels, R. M., Christ, C. L., "Solutions, Minerals and Equilibria," pp 98–99, Harper and Row, New York, N.Y., 1965.
(2) Garrels, R. M., Thompson, M. E., Siever, R., *Amer. J. Sci.*, **259**, 24 (1961).
(3) Greenwald, I., *J. Biol. Chem.*, **141**, 789 (1941).
(4) Greenwald, I., *J. Phys. Chem.*, **63**, 1328 (1959).
(5) Halla, F., Van Tassel, R., *ibid.*, **62**, 1135 (1958).
(6) Harned, H. S., Davis, R., Jr., *J. Amer. Chem. Soc.*, **65**, 2030 (1943).
(7) Harned, H. S., Sholes, S. R., *ibid.*, **63**, 1706 (1941).
(8) Hostetler, P. B., *J. Phys. Chem.*, **67**, 720 (1963).
(9) Kielland, J., *J. Amer. Chem. Soc.*, **59**, 1675 (1937).
(10) Latimer, W. M., "The Oxidation States of the Elements and Their Potentials in Aqueous Solutions," pp 30, 128, 316, Prentice-Hall, New York, N. Y., 1952.
(11) Näsänen, R., *Z. Phys. Chem.*, **A190**, 183 (1942).
(12) Raaflaub, J., *Helv. Chim. Acta*, **43**, 629 (1960).

RECEIVED for review October 25, 1968. Accepted January 17, 1971. Trade names and company names, when included, are for the convenience of the reader and do not imply preferential endorsement of a particular product or company over others.

---

# Solution-Crystal Equilibrium for Pyridine–Water System

ALFRED J. GLESSNER[1] and ALAN L. MYERS[2]
School of Chemical Engineering, University of Pennsylvania, Philadelphia, Pa. 19104

**New experimental data on the solid-liquid equilibrium of pyridine–water mixtures are reported. There is a pyridine hydrate which has an incongruent melting point at −28.6° C.**

The freezing-point data of Baud (*4*), Ewert (*9*), and Frédéric and Rayet (*9*) for pyridine-water mixtures are shown on Figure 1. If the pyridine-water system is a simple eutectic, then equilibrium is established between pure solid $i$ ($i = 1, 2$; pyridine is component 1, water is component 2) and liquid solution. The equilibrium condition for equality of fugacities is (*18*):

$$P_i^s = P_i^l \gamma_i x_i \qquad (1)$$

Equation 1 establishes two equilibrium lines $[x_1(T)$ and $x_2(T)]$ which should intersect at the eutectic composition.

The ratio of the vapor pressure of pure liquid to that of pure solid is given by the Schröder-Van Laar equation (*18*):

---

[1] Present address, Sun Oil Co., Marcus Hook, Pa.

[2] To whom correspondence should be addressed.

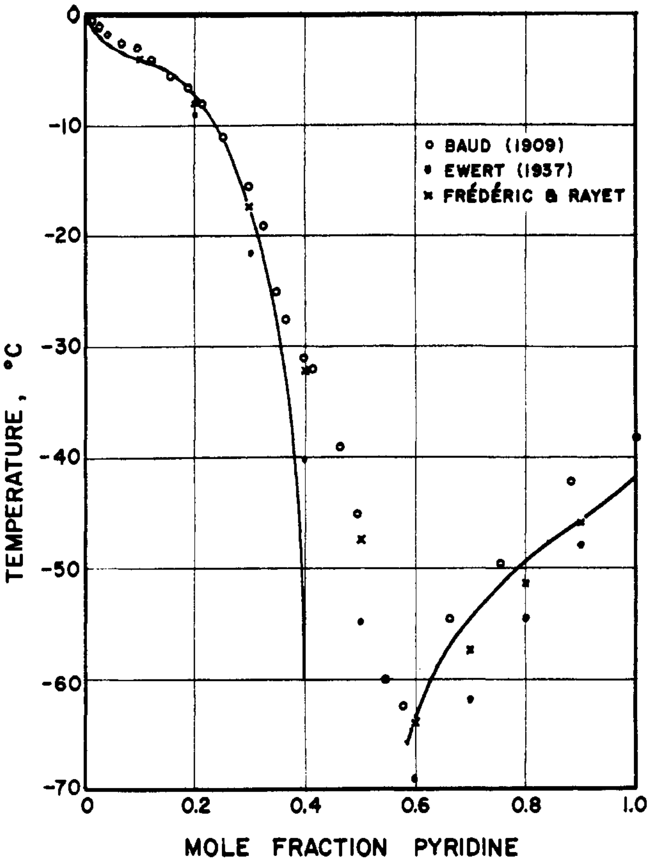

Figure 1. Freezing-point diagram for system pyridine–water

$$\ln \frac{P_i^l}{P_i^s} = \frac{\lambda_0}{RT_0}\left[\frac{T_0}{T} - 1\right] - \frac{\Delta c_p}{R}\left[\left(\frac{T_0}{T} - 1\right) - \ln\left(\frac{T_0}{T}\right)\right] \tag{2}$$

$\lambda_0$ is the heat of fusion at the triple point temperature ($T_0$). The $\Delta c_p$ is the change in specific heat upon fusion at $T_0$; Equation 2 is based upon the temperature invariance of $\Delta c_p$. These properties are tabulated in Table I for pyridine and water.

The activity coefficient ($\gamma_i$) is given by the excess Gibbs free energy ($\Delta g^e$) of the solution (*18*):

$$\ln \gamma_i = \frac{\partial}{\partial n_i}\left[(n_1 + n_2)\frac{\Delta g^e}{RT}\right]_{n_j,\,T} \tag{3}$$

Under the nonisothermal conditions of interest, the excess Gibbs free energy may be expressed (*6*) as a function of temperature and mole fraction:

$$\Delta g^e/RT = x_1 x_2 \bar{t}' C \bar{x} \tag{4}$$

where $C$ is an $m \times n$ matrix of constants; $\bar{t}$ is a column vector of $m$ elements:

$$\bar{t} = \begin{bmatrix} 1 \\ -1/T \\ \ln T \\ T \\ T^2/2 \\ \cdot \\ \cdot \\ T^{m-3}/(m-3) \end{bmatrix} \qquad \begin{aligned} t_1 &= 1 \\ t_2 &= -1/T \\ t_3 &= \ln T \\ t_i &= T^{i-3}/(i-3);\ i = 4, 5, \ldots, m \end{aligned} \tag{5}$$

The prime symbol denotes transposition, not differentiation. $\bar{x}$ is a column vector of $n$ elements:

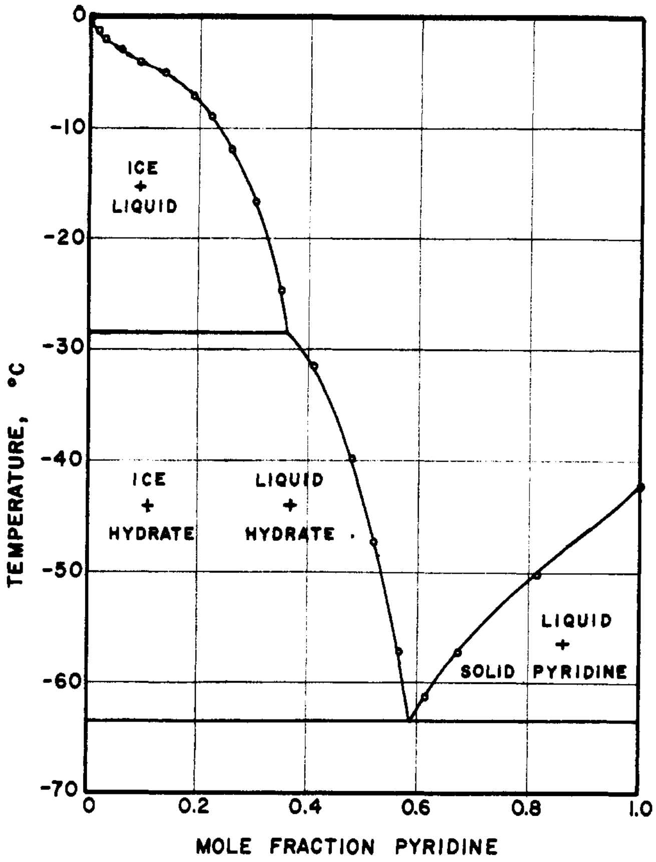

Figure 2. Experimental freezing-point diagram for system pyridine–water (this work)

$$\bar{x} = \begin{bmatrix} 1 \\ (x_1 - x_2) \\ (x_1 - x_2)^2 \\ \cdot \\ \cdot \\ (x_1 - x_2)^{n-1} \end{bmatrix} \qquad x_i = (x_1 - x_2)^{i-1} \tag{6}$$

The value of $C$ ($m = 4$, $n = 8$) is reported in Table II. The constants were evaluated using the vapor-liquid equilibrium data of Andon et al. (*3*) at 69.86° and 89.83° C;

Table I. Triple Point Data

| Substance | °K, $T_0$ | Cal/mol $\lambda_0$ | Cal/mol-°K, $\Delta c_p$ | Ref. |
|---|---|---|---|---|
| Pyridine | 231.49 | 1,979 | 6.99 | *16* |
| Water | 273.16 | 1,436 | 8.91 | *1* |

Table II. Transpose of Matrix (C) for Pyridine–Water Solutions

| | Column | | | |
|---|---|---|---|---|
| Row | 1 | °K, 2 | 3 | °K$^{-1}$, 4 |
| 1 | 242.379 | 8,127.5 | −40.3202 | 0.052300 |
| 2 | −96.073 | −3,257.5 | 15.9695 | −0.020699 |
| 3 | −176.127 | −5,821.1 | 29.6003 | −0.038389 |
| 4 | −3.087 | 52.5 | 0.5483 | −0.000725 |
| 5 | 622.797 | 19,241.6 | −105.0826 | 0.136314 |
| 6 | −260.025 | −8,055.1 | 43.8518 | −0.056881 |
| 7 | −463.736 | −14,098.9 | 78.4414 | −0.101763 |
| 8 | 55.688 | 1,577.1 | −9.5123 | 0.012340 |

the vapor-liquid equilibrium data of Ibl et al. (*14, 15*) at 30°, 50°, and 80° C; the enthalpy data of Wöycicka and Kurtyka (*19*) at 20° C; and the enthalpy data of Baud (*4*) at 12.5° C. The number of significant figures is large for the constants in Table II because calculations of $\Delta g^e$ using Equation 4 require the subtraction of numbers having nearly the same value.

Equation 1 was solved for $x_1(T)$ and $x_2(T)$ using Equations 2-4 and the value of $C$ in Table II. These calculated freezing point curves are given in Figure 1 and should be compared with the experimental points (*4, 9*). The comparison shows that the simple eutectic theory does not agree with the published data in the region from 35-60% pyridine. This discrepancy prompted the experimental work discussed in the following section.

## EXPERIMENTAL

We restudied the freezing point curves for pyridine-water. Our experimental results are reported in Table III. The temperature was measured with a quartz resonant-frequency thermometer manufactured by Hewlett-Packard, Dymec Model 2801A. The manufacturer's calibration of the thermometer was verified at the melting point of ice. The temperatures given in Table III are accurate within ±0.02° C. Two temperatures were recorded for each value of liquid composition: the freezing point temperature at which crystals first appeared upon cooling and the melting point temperature at which the last crystals melted upon warming. For each composition, the average of these two temperatures is the value recorded in Table III. Addition of the limit of error tabulated in Table III to the average temperature yields the freezing and melting point temperatures observed by us.

Our results for the phase diagram are plotted on Figure 2. Our data agree with the calculated freezing point curve discussed previously for the regions 0-36% and 59-100% pyridine. The data show that a new solid phase exists below -28.6° C.

## EVIDENCE OF A HYDRATE

The controversy in the literature over the existence of a pyridine hydrate is nearly a century old. In 1883, Goldschmidt and Constam (*10*) predicted a $C_5H_5N \cdot 3H_2O$ hydrate on the basis of an azeotrope of that composition obtained by distillation. Of course, it is now known that the existence of an azeotrope does not imply chemical bonding. Henry (*13*) concluded from an analysis of crystals that there is a $C_5H_5N \cdot H_2O$ hydrate. Gouy (*11*), on the basis of electrocapillary studies, concluded that there is a $C_5H_5N \cdot 3H_2O$ hydrate. Dunstan et al. (*8*) studied the viscosity for the pyridine-water system and, from discontinuities in the viscosity vs. concentration curves, predicted addition compounds of $2C_5H_5N \cdot 3H_2O$, $2C_5H_5N \cdot 5H_2O$, $C_5H_5N \cdot 5H_2O$, $C_5H_5N \cdot 10H_2O$, and $C_5H_5N \cdot 40H_2O$. Hartley et al. (*12*) also studied the viscosity-concentration curves but found no indication of the discontinuities mentioned by Dunstan et al. (*8*). Dunstan and Thole (*7*) repeated their study of the pyridine-water system and concluded, vaguely, that the question of whether the discontinuities exist is a matter of interpretation of results. Using thermal measurements, Baud (*5*) claimed the existence of two hydrates: $C_5H_5N \cdot 2H_2O$ and $C_5H_5N \cdot 6H_2O$. Later, Baud (*4*) reported a $C_5H_5N \cdot (1.9)H_2O$ hydrate on the basis of a crystal analysis and supported his claim with a discontinuity in the slope of the freezing point curve at this composition. Pariselle (*17*) criticized the work of Baud and was unable to verify the existence of a stable hydrate. Ewert (*9*) confirmed a discontinuity in the slope of the freezing point curve at a concentration of 35 mol % pyridine and inferred the existence of a $C_5H_5N \cdot 2H_2O$ hydrate. More recently, Andon et al. (*2*) examined the literature and concluded that there is no conclusive evidence for the existence of a stable hydrate.

Table III. Experimental Freezing Points for Mixtures of Pyridine-Water

| Mole fraction pyridine | Freezing point, ° C | Limit of error, ±° C |
|---|---|---|
| 0.0 | 0.00 | |
| 0.012 | -1.19 | 0.06 |
| 0.025 | -1.86 | 0.06 |
| 0.054 | -2.87 | 0.11 |
| 0.089 | -3.83 | 0.05 |
| 0.132 | -4.94 | 0.17 |
| 0.185 | -7.05 | 0.14 |
| 0.218 | -8.85 | 0.17 |
| 0.255 | -11.78 | 0.37 |
| 0.297 | -16.48 | 0.41 |
| 0.347 | -24.66 | 0.62 |
| 0.406 | -31.37 | 0.32 |
| 0.476 | -39.74 | 0.35 |
| 0.517 | -47.18 | 0.54 |
| 0.564 | -57.07 | 1.35 |
| 0.612 | -61.15 | 0.60 |
| 0.669 | -57.15 | 0.42 |
| 0.811 | -50.06 | 0.20 |
| 0.996 | -42.18 | 0.11 |
| 1.0 | -41.67 | |

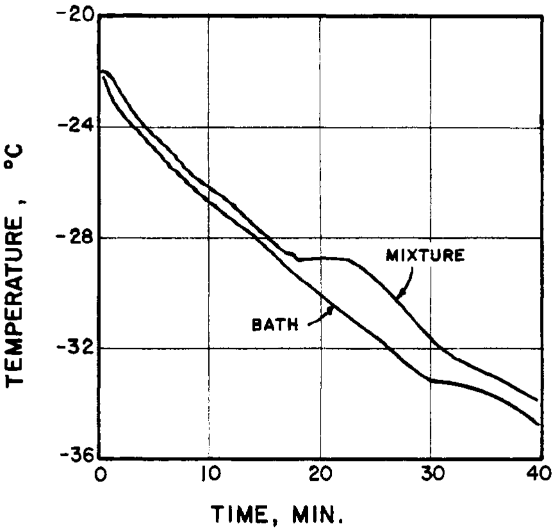

Figure 3. Cooling curve for pyridine-water mixture

Mole fraction pyridine = 0.347

We obtained evidence for the existence of a hydrate by observing the evolution of heat during its formation. A typical cooling curve is shown on Figure 3. Ice crystals appeared at -25.24° C but this is not noticeable in Figure 3 because of the relatively small amount of heat evolved. The incongruent melting point of the hydrate is -28.6 ± 0.2° C.

For the measurement of hydrate-liquid equilibria, it was necessary to seed the liquid sample with hydrate crystals in order to prevent excessive supercooling. Seeding with ice crystals did not prevent supercooling.

An X-ray diffraction study was made. For samples containing less than 36 mol % pyridine, ice crystals are formed first as shown in Figure 2. The X-ray diffraction pattern for ice was observed for these samples even at -50° C. But for a 40 mol % pyridine mixture at -50° C, the diffraction pattern for ice is replaced by a new pattern, that of the hydrate.

In Figure 2, the vertical line (below -28.6° C) separating the ice-hydrate system from the liquid-hydrate system is

Table IV. Thermodynamic Properties of Hydrate, $C_5H_5N \cdot nH_2O$

| $n$ | −28.6° C, $K$ | Cal, $\Delta H^0$(l) | Cal, $\Delta H^0$(s) |
|---|---|---|---|
| 3 | 7.4 | −7,800 | −2,200 |
| 4 | 9.9 | −11,200 | −4,400 |
| 5 | 13.4 | −14,700 | −6,700 |

absent because the hydrate composition is unknown. To the left of this vertical line the mixture is solidified; to the right the system consists of solid hydrate and liquid in equilibrium. But it is difficult to distinguish between the dry solid and the two-phase mixture of liquid and solid.

For addition compounds with a congruent melting point, it is possible to determine the composition of the hydrate with high accuracy by studying cooling curves at different compositions. But for the pyridine–water system there is an incongruent melting point; on cooling, ice forms first. At the incongruent melting point (−28.6° C), some or all of this ice must be transformed to solid hydrate. This transformation is a slow process. Consequently our thermal analysis was difficult to interpret and inconclusive.

The composition of the hydrate was studied by analyzing crystals which were filtered from solution at −50° C. The separation of the solid hydrate is difficult because of occlusion of liquid in the crystals. We were able to separate crystals with the composition of 27.5 mol % pyridine. Therefore the hydrate composition is equal to or less than 27.5 mol % pyridine.

## THERMODYNAMIC PROPERTIES OF HYDRATE

The thermodynamic properties of the hydrate can be calculated from the experimental freezing-point curve of the hydrate from −28.6° to −63° C (see Figure 2). The chemical reaction is:

$$C_5H_5N(l) + nH_2O(l) \rightleftarrows C_5H_5N \cdot nH_2O(s) \qquad (7)$$

The equilibrium constant for this reaction is:

$$K = 1/a_1 a_2^n \qquad (8)$$

The standard states are the pure solid for the hydrate (unit activity) and the pure liquids for pyridine and water. The activity in the liquid mixture is given by

$$a_i = \gamma_i x_i \qquad (9)$$

Equilibrium constants were calculated by means of Equation 8 and the experimental composition of the equilibrium liquid. Activity coefficients in Equation 9 were evaluated using Equations 3 and 4 and the value of $C$ in Table II. The value of $K$ at the incongruent melting point of the hydrate is reported in Table IV for several possible values of $n$.

The standard heat of reaction for Equation 7 may be obtained from the van't Hoff equation:

$$\Delta H^0(l) = -R[d \ln K/d(1/T)] \qquad (10)$$

$\Delta H^0$(l) is the enthalpy change for the formation of the solid hydrate from the pure liquids. Since a plot of ln $K$ vs. $(1/T)$ from −28.6° to −63° C is a straight line, $\Delta H^0$(l) was taken to be a constant. Values of $\Delta H^0$(l), calculated by Equation 10, are reported in Table IV.

The heat of formation of the hydrate from the pure solids [$\Delta H^0$(s)] is easier to interpret than $\Delta H^0$(l). The two enthalpy differences are related by:

$$\Delta H^0(s) = \Delta H^0(l) + \Lambda^0 \qquad (11)$$

$\Lambda^0$, the heat of fusion of the pure solids (water and pyridine), is given by:

$$\Lambda^0 = \lambda_1 + n\,\lambda_2 \qquad (12)$$

The molar heats of fusion of pure pyridine ($\lambda_1$) and pure water ($\lambda_2$) were estimated by:

$$\lambda = \lambda_0 + \Delta c_p (T - T_0) \qquad (13)$$

and the values of $\lambda_0$ and $\Delta c_p$ given in Table I. Values for $\Delta H^0$(s), calculated by means of Equations 11–13, are given in Table IV for several possible values of $n$.

## NOMENCLATURE

$a_i$ = activity of *i*th component
$c_p$ = molar specific heat at constant pressure
$C$ = $m \times n$ matrix of constants, Equation 4
$g$ = molar Gibbs free energy, cal/mol
$H$ = enthalpy, cal
$K$ = chemical equilibrium constant
$n_i$ = number of moles of *i*th component
$n$ = number of water molecules, Equation 7
$P_i$ = vapor pressure of *i*th component
$R$ = gas constant
$\bar{t}$ = a vector, Equation 5
$T$ = absolute temperature, ° K
$\bar{x}$ = a vector, Equation 6
$x_i$ = mole fraction of *i*th component
$\gamma_i$ = activity coefficient of *i*th component in liquid phase
$\Lambda$ = heat of fusion, cal
$\lambda$ = molar heat of fusion, cal/mol

### Superscripts

$e$ = excess thermodynamic property
l = liquid state
s = solid state
0 = pure state

### Subscripts

0 = triple point
1 = pyridine
2 = water
$i$ = *i*th component

## LITERATURE CITED

(1) American Institute of Physics Handbook, 4-142, McGraw-Hill, New York, N. Y., 1957.
(2) Andon, R. J. L., Cox, J. D., Herington, E. F. G., *Discuss. Faraday Soc.*, **15**, 168 (1953).
(3) Andon, R. J. L., Cox, J. D., Herington, E. F. G., *Trans. Faraday Soc.*, **53**, 410 (1957).
(4) Baud, M. E., *Bull. Soc. Chim. France*, **5**, 1022 (1909).
(5) Baud, M. E., *Compt. Rend.*, **148**, 96 (1909).
(6) Carnahan, B., Myers, A. L., "Thermodynamic Excess Functions of Liquid Mixtures," in preparation.
(7) Dunstan, A. E., Thole, F. B., *J. Chem. Soc.*, **93**, 561 (1908).
(8) Dunstan, A. E., Thole, F. B., Hunt, J. S., *ibid.*, **91**, 1728 (1907).
(9) Ewert, M., *Bull. Soc. Chim. Belges*, **46**, 90 (1937).
(10) Goldschmidt, H., Constam, E. J., *Deut. Chem. Gesells.*, **16**, 2976 (1883).
(11) Gouy, M., *Ann. Chim. Phys.*, *Series 8*, **9**, 75 (1906).
(12) Hartley, H., Thomas, N. G., Appelbey, M. P., *J. Chem. Soc.*, **93**, 538 (1908).
(13) Henry, L., *Bull. Acad. Roy. Belg.*, *Series 3*, **27**, 448 (1894).
(14) Ibl, N. Von, Dändliker, G., Trümpler, G., *Chem. Eng. Science*, **5**, 193 (1956).
(15) Ibl, N. Von, Dändliker, G., Trümpler, G., *Helv. Chim. Acta*, **37**, 1661 (1954).
(16) McCullough, J. P., Douslin, D. R., Messerly, J. F., Hossenlopp, I. A., Kincheloe, T. C., Waddington, Guy, *J. Amer. Chem. Soc.*, **79**, 4289 (1957).
(17) Pariselle, M., *Compt. Rend.*, **172**, 673 (1921).
(18) Prigogine, I., Defay, R., Everett, D. H., "Chemical Thermodynamics," pp 357, 368-83, Longmans, Green, London, 1954.
(19) Wóycicka, M., Kurtyka, Z., *Bull. Acad. Polon. Sci., Ser. Sci. Chim.*, **13**, 469 (1965).

RECEIVED for review July 24, 1969. Accepted January 18, 1971.